Ancestral SARS-CoV-2 immune imprinting persists on RBD but not NTD after sequential Omicron infections

Zuowei Wang[1,2], Ling Li[1,2], Ruiping Du[1], Xixian Chen[1], Yi Sun[1], Rongrong Qin[1], Yunjian Li[1], Hualong Feng[1], Lin Hu[1], Xuanyi Chen[1], Maosheng Lu[1], Liwei Jiang[1,*], Teng Zuo[1,*]

[1]Laboratory of Immunoengineering, Institute of Health and Medical Technology, Hefei Institutes of Physical Science, Chinese Academy of Sciences, Hefei 230031, China

[2]These authors contributed equally to this work

*Correspondence: jlw0531@cmpt.ac.cn (L.J.); zuot@cmpt.ac.cn (T.Z.)

Summary

Whether Omicron exposures could overcome ancestral SARS-CoV-2 immune imprinting remains controversial. Here we analyzed B cell responses evoked by sequential Omicron infections in vaccinated and unvaccinated individuals. Plasma neutralizing antibody titers against ancestral SARS-CoV-2 and variants indicate that immune imprinting is not consistently induced by inactivated or recombinant protein vaccines. However, once induced, immune imprinting is not countered by successive Omicron challenges. We compared binding specificities, neutralizing capacities, developing origins and targeting epitopes of monoclonal antibodies from individuals with or without immune imprinting. Although receptor-binding domain (RBD) and N-terminal domain (NTD) of spike are both primary targets for neutralizing antibodies, immune imprinting only shapes antibody responses to RBD by impeding the production of Omicron-specific neutralizing antibodies while facilitating the development of broadly neutralizing antibodies. We propose that immune imprinting can be either neglected by NTD-based vaccines to induce variant-specific antibodies or leveraged by RBD-containing vaccines to induce broadly neutralizing antibodies.

Highlights

- Immune imprinting is not consistently induced by vaccination
- Repeated Omicron infections could not counter immune imprinting
- Immune imprinting shapes antibody responses to RBD but not NTD
- Immune imprinting leads to broadly neutralizing antibodies

34 **Introduction**

35 Immunological memory is a hallmark of adaptive immunity, which consists of humoral
36 and cellular immunity[1]. Upon primary exposure to an antigen, humoral immune
37 responses typically start from priming of naive B cells through cognate interaction
38 between B cell receptor (BCR) and antigen in follicles of secondary lymphoid organs[2].
39 Primed B cells migrate to the border between B cell follicle and T cell zone, where they
40 encounter activated CD4 T cells. Cognate T-B interaction leads to clonal expansion of
41 B cells and formation of germinal centers (GCs). Within GCs, B cells undergo somatic
42 hypermutation (SHM) on variable region of BCR to generate a pool of mutated B cells,
43 which are then selected based on their affinities to the antigen. After repeated rounds
44 of mutation and selection, affinity-matured GC B cells differentiate into plasmablasts
45 (PBs), plasma cells (PCs) or memory B cells. PB/PCs constantly secret antibodies and
46 maintain high levels of serum antibodies for months to years. Meanwhile, memory B
47 cells circulate throughout the body until they encounter cognate antigens. Activated
48 memory B cells rapidly differentiate into PB/PCs to secret antibodies, or to a lesser
49 extent, into GC B cells to undergo another round of affinity maturation[3].

50 As the basic principle of long-term immune protection against pathogens after infection
51 or vaccination, immunological memory ensures much faster and stronger immune
52 responses upon antigen re-exposure[1]. However, the effects of immunological memory
53 could be undesirable when antigens in prior and subsequent exposures are
54 heterologous but antigenically related. One example of such scenario is that
55 individuals' antibody responses against influenza viruses are largely biased towards

56 the predominant strains in their early lives[4]. This phenomenon is referred to as original
57 antigenic sin or immune imprinting, which describes the effects of immunity elicited by
58 prior antigen exposures on subsequent immune responses to antigenically related
59 antigens.
60 Since the outbreak of COVID-19 pandemic, the ancestral SARS-CoV-2 has kept
61 evolving and generated hundreds of thousands of variants. Among them, Omicron
62 emerged in November 2021 and accumulated more than 30 mutations on spike, the
63 target of neutralizing antibodies[5]. Over the past two and a half years, the predominant
64 strains have been rapidly iterated by Omicron-derived variants, including BA.1, BA.2,
65 BA.4, BA.5, BQ.1, XBB.1.5, XBB.1.16, XBB.1.9, EG.5.1 and BA.2.86. These variants
66 exhibit unprecedented neutralization evasion from antibodies elicited by ancestral
67 SARS-CoV-2 infection or vaccines based on ancestral SARS-CoV-2 [6-11]. Consequently,
68 several waves of infection by Omicron variants have occurred and updated vaccines
69 have been developed to match those variants [12-14].
70 Analysis of B cell responses in individuals who experienced breakthrough infection of
71 Omicron variants or received Omicron booster vaccines demonstrates the induction of
72 immune imprinting by ancestral SARS-CoV-2[15-20]. Moreover, the imprinted antibody
73 responses display substantially reduced neutralizing activities against later Omicron
74 variants compared with ancestral SARS-CoV-2 and earlier Omicron variants,
75 highlighting that immune imprinting may impede the generation of neutralizing
76 antibodies against future SARS-CoV-2 variants or other related viruses[21]. Notably, a
77 recent study reported that sequential Omicron exposures could overcome immune

78 imprinting and induce a large portion of *de novo* Omicron-specific antibodies[22]. In
79 contrast, other studies concluded that a single exposure to antigenically distant
80 XBB.1.5 or double exposures to Omicron variants rarely elicited Omicron-specific
81 antibody responses in the presence of immune imprinting[23-25]. Therefore, it is
82 controversial whether Omicron exposures could override ancestral SARS-CoV-2
83 immune imprinting.
84 In this study, we compared human B cell responses elicited by sequential Omicron
85 infections in the presence or absence of ancestral SARS-CoV-2 immune imprinting.
86 By measuring plasma neutralizing antibody titers against ancestral SARS-CoV-2 and
87 variants, we find that immune imprinting is not consistently induced by inactivated or
88 recombinant protein vaccines. However, once induced, immune imprinting is not
89 countered by repeated Omicron exposures. Comprehensive analysis of monoclonal
90 antibodies from individuals with or without immune imprinting demonstrates that RBD
91 and NTD are both primary targets for neutralizing antibodies, whereas only RBD-
92 specific antibody responses are imprinted. Consequently, Omicron-specific
93 neutralizing antibodies to RBD are hindered while broadly neutralizing antibodies to
94 RBD are elicited. These findings provide new insights into the development of next-
95 generation SARS-CoV-2 vaccines.

96 **Results**

97 **Sequential Omicron infections could not overcome ancestral SARS-CoV-2**
98 **immune imprinting induced by inactivated or recombinant RBD vaccines.**

99 To examine whether Omicron exposures could overcome ancestral SARS-CoV-2
100 immune imprinting, we collected peripheral blood from 12 donors of sequential
101 Omicron infections (Figure 1A). They were first infected in December 2022 or January
102 2023, when BA.5 and BF.7 were predominant strains[26]. Around half a year later, they
103 were infected again when XBB lineages (XBB*) were predominant strains[27]. Before the
104 infections, Donor A and B were not administrated with any vaccines based on ancestral
105 SARS-CoV-2, while the other donors received two or three doses of inactivated
106 vaccine or recombinant RBD vaccine or in combination.
107 We measured plasma neutralizing antibody titers against a panel of 18 pseudoviruses
108 bearing spikes from ancestral SARS-CoV-2 (WT), Alpha, Beta, Gamma, Delta, BA.1,
109 BA.4/5, BA.2.75, XBB, XBB.1.5, EG.5, EG.5.1, FL.1.5, FL.1.5.1, HK.3, BA.2.86, JN.1
110 and SARS-CoV-1 (Figure S1A). Donor A-D show poor or lower neutralizing titers
111 against earlier SARS-CoV-2 strains from WT to BA.1 while higher titers against strains
112 from BA.4/5 to HK.3 (Figure 1B). As Donor A and B were unvaccinated, their patterns
113 represent antibody responses induced by sequential Omicron exposures in the
114 absence of immune imprinting. Despite the fact that Donor C and D were vaccinated,
115 they display similar patterns with Donor A and B, suggesting that immune imprinting is
116 not induced by vaccination in Donor C and D. Donor E-K maintain higher titers against
117 earlier strains from WT to BA.2.75 while lower titers against XBB and later strains,
118 indicating the presence of immune imprinting in these individuals (Figure 1C). Different
119 from above donors, Donor L exhibits a quite chaotic pattern of neutralizing titers and
120 thus is excluded for further analysis (Figure S1B).

121 We compared neutralizing titers of Donor A-D (referred to as unimprinted group, G1)
122 and Donor E-K (referred to as imprinted group, G2) (Figure 1D). For early strains from
123 WT to BA.1, imprinted group has significantly higher titers than unimprinted group. On
124 the contrary, for more recent Omicron variants, including XBB, XBB.1.5, EG.5, EG.5.1,
125 FL.1.5 and HK.3, unimprinted group surpasses the imprinted group. Taken together,
126 these data suggest that immune imprinting is not consistently induced by vaccination.
127 However, once induced, immune imprinting is not countered by sequential Omicron
128 infections.

129 **Immune imprinting leads to more frequent cross-reactive antibodies to RBD but**
130 **not NTD**

131 To decipher the effects of immune imprinting on human B cell responses elicited by
132 sequential Omicron infections, we moved on to isolate and characterize monoclonal
133 antibodies (mAbs) from those donors. As they were sequentially exposed to BA.5/BF.7
134 and XBB*, we sorted single memory B cells or plasmablasts with XBB.1.5 spike as bait
135 (Figure S2). After cloning antibody variable regions from single cells into corresponding
136 antibody-expressing vectors, we transfected HEK293T cells with paired plasmids and
137 collected supernatant for ELISA and neutralization assay. The supernatant was tested
138 against spike (S), S1, RBD, NTD and S2 of XBB.1.5 and WT by ELISA, and tested
139 against XBB.1.5 and WT pseudoviruses by neutralization assay (Figure 2A). In total,
140 we identified 364 clones positive for XBB.1.5 spike from Donor A, B, C, D, E, F, G, I, J
141 and K. The proportions of antibodies against each domain vary in a wide range and no
142 significant differences are observed between unimprinted group (G1) and imprinted

143 group (G2) (Figure 2B). With 50% as cutoff for neutralization of supernatant, 84 clones
144 were identified as neutralizing antibodies against XBB.1.5 or WT or both (Figure 2A,
145 B). Notably, cross-neutralizing antibodies are all from imprinted group (Figure 2A). In
146 addition, the vast majority of neutralizing antibodies target either RBD or NTD and
147 there are no significant differences between the two groups (Figure 2B).
148 We further analyzed the frequency of cross-reactive antibodies (XBB.1.5^{+} WT^{+}) (Figure
149 2C, D). Most S2-specific antibodies are cross-reactive, which should be due to the
150 conservation of this domain. For NTD-specific antibodies, the frequencies range from
151 0 to 50% and there is no difference between G1 and G2. In contrast, for RBD-specific
152 antibodies, G2 has remarkably higher frequency than G1, which represents recall of
153 cross-reactive memory B cells induced by vaccination. Overall, these results indicate
154 that immune imprinting mainly influences antibody responses to RBD after sequential
155 Omicron infections.

156 **Immune imprinting facilitates the development of broadly neutralizing**
157 **antibodies against RBD**

158 To determine the effects of immune imprinting on neutralizing antibodies, we purified
159 RBD- or NTD-specific mAbs with supernatant neutralization above or close to 50%. A
160 total number of 87 mAbs, including 16 RBD-specific and 32 NTD-specific mAbs from
161 G1 and 33 RBD-specific and 6 NTD-specific mAbs from G2, were tested against a
162 panel of SARS-CoV-2 pseudoviruses (Figure 3A). Similar to the neutralization patterns
163 of plasma from G1, RBD-specific mAbs from G1 (G1-RBD) poorly neutralize early
164 strains from WT to BA.1 while potently neutralize later Omicron variants. RBD-specific

mAbs from G2 can be divided into two subgroups according to their neutralization patterns. One subgroup resembles mAbs from G1-RBD in neutralization pattern and is named as non-WT-neutralizing (Abbreviated as non-WT-neut). The other subgroup replicates the neutralization patterns of plasma from G2 and is termed as WT-neutralizing (Abbreviated as WT-neut). It is worth mentioning that there are several broadly neutralizing antibodies in this group, including KXD-E1, KXD-F3, KXD-F1, KXD-G10 and KXD-G5. Most NTD-specific mAbs are able to neutralize BA.4/5, BQ.1, XBB, XBB.1.5, EG.5.1 and HK.3, and the patterns are similar between G1 and G2.

Regarding to the neutralizing potency (IC50s) against different strains, mAbs from G1-RBD are more potent to BA.4/5 than later variants whereas mAbs from G2-RBD-non-WT-neut exhibit similar neutralizing activity against BA.4/5 and later strains (Figure S3A). Antibodies from G2-RBD-WT-neut have equivalent potency to early strains from WT to BA.4/5 while decreased potency to later variants (Figure S3A). Different from RBD-specific mAbs, NTD-specific mAbs from both G1 and G2 are most potent to XBB and XBB.1.5 (Figure S3B).

We compared the neutralizing potency of mAbs from different groups against the same strain (Figure 3B,3C). Overall, mAbs from G1-RBD have similar neutralizing potency with mAbs from G2-RBD-non-WT-neut. However, mAbs from G1-RBD are more potent than mAbs from G2-RBD-WT-neut against variants from BA.4/5 to JN.1 except BA.2.75 and XBB. On the other hand, NTD-specific mAbs from both groups have analogous potency against all tested strains except HK.3. These data further confirm that antibody responses to RBD while not NTD are affected by immune imprinting.

187 Moreover, the imprinted RBD-specific antibodies tend to have broadly neutralizing
188 activity although they generally show suboptimal neutralizing potency against Omicron
189 variants.

190 **Repeated Omicron infections induce de novo Omicron-specific antibody**
191 **responses in the presence of immune imprinting**

192 To examine whether repeated Omicron infections could induce de novo antibody
193 responses from naïve B cells in the presence of immune imprinting, we move on to
194 investigate the origins of neutralizing mAbs from each group. In published literatures,
195 it is generally assumed that cross-reactive antibodies derive from memory B cells
196 induced by WT whereas omicron-specific antibodies originate from naïve B cells
197 activated by Omicron[22-25]. However, these assumptions remain to be confirmed by
198 experiments to exclude possibilities that memory B cells induced by WT may lose
199 cross-reactivity and Omicron-specific naïve B cells may develop cross-reactivity during
200 affinity maturation. Here, we constructed germline versions of representative mAbs
201 from each group and tested their binding to a panel of spikes expressed on HEK293T
202 cells by FACS (Figure 4A). Germline antibodies from G1-RBD, G2-RBD-non-WT-neut,
203 G1-NTD and G2-NTD bind Omicron spikes but not WT spike. Oppositely, germline
204 antibodies from G2-RBD-WT-neut mostly recognize WT spike but not Omicron spikes.
205 These data confirm that mAbs from G1-RBD, G2-RBD-non-WT-neut, G1-NTD and G2-
206 NTD are de novo antibodies induced by Omicron, whereas mAbs from G2-RBD-WT-
207 neut are recalled antibodies initially induced by WT.

208 Correlated with their origins, mAbs from G2-RBD-WT-neut show higher mutation levels
209 than other mAbs, which reflects extensive affinity maturation sequentially driven by WT
210 and Omicron (Figure 4B). On the other hand, we also analyzed the repertoire of each
211 group (Figure 4C and Table 1). In G2-RBD-WT-neut group, IGHV1-18 and IGLV1-44
212 are most frequent as a consequence of B cell clonal expansion in Donor J. Moreover,
213 IGHV3-53, IGHV3-66 and IGHV1-69, which have been identified as frequent VH genes
214 for RBD-specific antibodies from individuals exposed to WT spike[28,29], are frequently
215 used in G2-RBD-WT-neut but not in G1-RBD and G2-RBD-non-WT-neut. For NTD-
216 specific antibodies, IGHV4-39 is most frequently used and is identified from multiple
217 donors in both groups. Therefore, these IGHV4-39 antibodies can be taken as a class
218 of public antibody against NTD. In sum, these data suggest that repeated Omicron
219 exposures could induce de novo antibody responses to RBD and NTD in the presence
220 of immune imprinting.

221 **Omicron-specific and WT-cross-reactive antibodies recognize similar epitopes**

222 To determine whether de novo antibody responses induced by repeated Omicron
223 infections recognize distinct epitopes compared with WT-cross-reactive antibodies, we
224 performed competition ELISA (Figure 5A, 5B). Three broadly neutralizing antibodies
225 targeting RBD, including BD55-1205, BD56-1854 and BD55-5483 were taken as
226 reference[30]. A major cluster is formed by the majority of RBD-specific antibodies. Most
227 antibodies in this cluster also compete with BD55-1205, BD56-1854 and ACE2.
228 Outside the major cluster, a minor cluster is formed by 6 antibodies. They compete
229 with BD55-5483 but not with BD55-1205, BD56-1854 and ACE2. The rest 3 RBD-

specific antibodies do not exhibit apparent competition with other antibodies or ACE2. On the other hand, NTD-specific antibodies show competition with each other and form a single cluster, suggesting that NTD-specific neutralizing antibodies target a supersite. Taken together, these data provide explanation for the suppressed Omicron-specific antibody responses to RBD in the presence of immune imprinting.

Discussion

In this study, we compared B cell responses evoked by sequential Omicron infections in individuals vaccinated or unvaccinated with inactivated or recombinant RBD vaccines. Unexpectedly, two vaccinees show no hints of immune imprinting, according to their polyclonal and monoclonal antibody responses against ancestral SARS-CoV-2 and variants. Therefore, they are classified into unimprinted group along with two unvaccinated individuals throughout this study. Considering the factor of individual variations, we believe that this classification is more reasonable than simply grouping the cohorts based on antigen exposure history, especially for cohorts with limited size. We speculate that no immune imprinting in these two individuals is probably due to weak immune responses stimulated by vaccination. Moreover, whether this phenomenon is common remains to be determined with larger cohorts.

In contrast to individuals without immune imprinting, individuals with immune imprinting have lower plasma neutralizing antibody titers against multiple Omicron variants after XBB, along with more frequent WT-cross-reactive antibodies and less frequent Omicron-specific antibodies to RBD. Therefore, we conclude that immune imprinting induced by inactivated or recombinant RBD vaccines is not countered by sequential

252 Omicron infections, which is inconsistent to a study performed by Yisimayi et al[22]. We
253 suppose this contradiction is due to following factors. First, the infections were
254 sequentially caused by BA.1/BA.2 and BA.5/BF.7 in their study whereas by BA.5/BF.7
255 and XBB* in our study. We notice that individuals with or without immune imprinting
256 have equivalent plasma neutralizing antibody titers to BA.4/5 and BA.2.75. Moreover,
257 individuals with immune imprinting show unaffected neutralizing titers against early
258 Omicron variants including BA.1, BA.2.75 and BA.4/5 compared with WT. These data
259 suggest that immune imprinting does not compromise antibody responses to early
260 Omicron variants after repeated Omicron exposures. Second, all vaccinees were
261 considered as imprinted in their study while two vaccinees were taken as unimprinted
262 in our study. As vaccinees without immune imprinting are able to generate abundant
263 Omicron-specific antibodies, excluding them from imprinted cohort may lead to more
264 clear results.
265 A major finding of our study is that antibody responses to NTD are not affected by
266 immune imprinting. As immunological memory and cross-reactivity are the basis of
267 immune imprinting[31], one possible explanation for this finding is that NTD is less
268 immunogenic than RBD because of its extensive glycan shielding[32,33], and thus few
269 NTD-specific memory B cells are induced. Another possible explanation is that NTD-
270 specific memory B cells induced by WT are not cross-reactive to Omicron variants.
271 However, consistent with previous studies[34-39], our results argue that NTD is highly
272 immunogenic and able to elicit antibodies cross-reactive to XBB.1.5 and WT, which
273 meet the preconditions for immune imprinting. Therefore, the mechanisms for the

274 unimprinted antibody responses to NTD remain to be explored.

275 Similar to previous studies[15-18,20,22-24], we prove that immune imprinting persistently
276 shapes antibody responses to RBD. As a result, RBD-specific antibodies can be
277 divided into two groups: WT-cross-reactive antibodies and Omicron-specific antibodies.
278 Compared with Omicron-specific antibodies, WT-cross-reactive antibodies tend to
279 have broader neutralization spectrum. For example, KXD-F1 neutralize all tested
280 pseudoviruses from WT to JN.1 with IC50s ranging from 0.006 to 0.084 μg/ml. As
281 germlines of those WT-cross-reactive antibodies generally have limited breadth, there
282 is no doubt that the breadth of WT-cross-reactive antibodies is attributed to affinity
283 maturation. However, the underlying mechanisms are not fully understood. According
284 to the model of affinity maturation in GCs, it is possible that WT-cross-reactive memory
285 B cells become Omicron-specific after affinity maturation. By comparing the binding
286 specificities of paired germline and mature antibodies, we find that all WT-reactive
287 germline antibodies consistently recognize WT spike after affinity maturation, which
288 negate the possibility like our previous study[40]. Oppositely, it is also possible that
289 Omicron-specific naïve B cells may become cross-reactive after affinity maturation.
290 However, we have not found evidence to support the possibility, despite that fact that
291 infection or vaccination with WT could elicit broadly neutralizing antibodies against
292 Omicron variants[30,41-43]. More studies are required to solve these puzzles on affinity
293 maturation.

294 Currently, ancestral SARS-CoV-2 immune imprinting has been acknowledged as a
295 great barrier for vaccine update. According to our findings, we propose that NTD-based

296 vaccines could be designed to bypass immune imprinting, since NTD is also a major
297 target of neutralizing antibodies. On the other hand, vaccines containing RBD could
298 be designed to leverage the potential of immune imprinting in eliciting broadly
299 neutralizing antibodies.

300 **Limitations of the study**

301 Although we included unvaccinated and vaccinated individuals in this study, both
302 cohorts are relatively limited in size. Moreover, the numbers of antibodies cloned from
303 different individuals are not equivalent, with a range from 6 to 89. In addition, only
304 XBB.1.5 spike was used to stain the B cells for single cell sorting, and thus the
305 frequencies of cross-reactive and Omicron-specific B cells were not determined by
306 FACS.

307

308 **Materials and methods**

309 **Ethics statement**

310 This study was approved by the Ethics Committee of Hefei Institutes of Physical
311 Science, Chinese Academy of Sciences (Approval Number: YXLL-2023-47). All donors
312 provided written informed consent for collection of information, analysis of plasma and
313 PBMCs, and publication of data generated from their samples.

314 **Human samples**

315 Peripheral blood samples were collected from 12 donors (Figure1A). Plasma and
316 peripheral blood mononuclear cells (PBMCs) were separated from blood by Ficoll
317 density gradient centrifugation.

318 **Cell lines**

319 HEK293T cells expressing human ACE2 (HEK293T-hACE2) were kindly provided by
320 Prof. Ji Wang at Sun Yat-Sen University. HEK293T cells were from ATCC. HEK293T
321 and HEK293T-hACE2 cells were cultured in DMEM with 10% fetal bovine serum (FBS,
322 VivaCell, Shanghai, China, C04001) and 1% penicillin/streptomycin (pen/strep).
323 FreeStyle 293F cells (Thermo Fisher Scientific) were cultured in SMM 293-TII
324 Expression Medium (Sino Biological Inc., M293TII). All cells were maintained in a 37˚C
325 incubator at 5% CO_2

326 **Protein expression and purification**

327 The genes encoding the ectodomain of SARS-CoV-2 spike including WT and XBB.1.5
328 were constructed with foldon trimerization motif, His tag, tandem strep-tag II and FLAG
329 tag at C-terminal. The genes encoding the S1, NTD and RBD of WT and XBB.1.5 were

330 constructed with a strep-tag II at C-terminal. The genes encoding the S2 of WT and
331 XBB.1.5 were constructed with a His tag at C-terminal. Spike trimer, S1, S2, NTD and
332 RBD were expressed in the FreeStyle 293F cells and purified by Streptactin Agarose
333 Resin 4FF (Yeasen, 20495ES60) or Ni-NTA Agarose (Qiagen, 30210).

334 **Spike-specific Single B cell sorting and PCR**

335 PBMCs were incubated with 200nM XBB.1.5 spike for 30 min at 4˚C. After wash, they
336 were stained with cell-surface antibodies: CD3-BV510 (BioLegend, 317331), CD19-
337 PE/Cy7 (BioLegend, 302215), CD27-APC (BioLegend, 356409), CD38-APC/Cy7
338 (BioLegend, 356615), human IgM-AF700 (BioLegend, 314537), human IgD-
339 perCP/Cy5.5 (BioLegend, 348207), anti-His-AF488 (Proteintech, CL488-66005), anti-
340 FLAG-PE (BioLegend, 637309) and DAPI. The stained cells were washed with FACS
341 buffer (PBS containing 2% FBS) and resuspended in 500μl FACS buffer. Spike-specific
342 single B cells were gated as $DAPI^{-}CD3^{-}CD19^{+}CD27^{+}IgD^{-}His^{+}FLAG^{+}$ and sorted into
343 96-well PCR plates containing 4μl lysis buffer (0.5×PBS, 0.1M DTT and RNase
344 inhibitor) per well. After reverse transcription reaction, variable regions of heavy and
345 light chains were amplified by nested PCR and cloned into human IgG1 expression
346 vectors. Plasmids for paired heavy and light chains were co-transfected into HEK293T
347 cells or FreeStyle 293F cells. Antibodies were purified with Protein A magnetic beads
348 (GenScript, L00273).

349 **ELISA**

350 Spike, S1, S2, NTD or RBD were coated onto 96-well ELISA plates (100 ng/well) and
351 incubated at 4˚C overnight. After blocking with PBS containing 10% FBS, HEK293T

352 supernatant was added to the wells and incubated at 37˚C for 1hr. HRP-conjugated
353 goat anti-human IgG antibodies (Zen-bio, 550004; 1:2000 dilution) were added to the
354 wells and incubated at 37˚C for 1hr. TMB substrate (Sangon Biotech, E661007-0100)
355 was added to the wells and incubated at room temperature for 5 mins. The reaction
356 was stopped by TMB Stop Solution (Sangon Biotech, E661006-0500) and absorbance
357 at 450 nm was measured.

358 **Pseudovirus neutralization assay**

359 To generate pseudoviruses, HEK293T cells were transfected with psPAX2, pLenti-
360 luciferase and spike-encoding plasmids using polyetherimide (PEI). Supernatants with
361 pseudoviruses were collected 48hrs after transfection. 3-fold serially diluted plasma
362 (starting at 1:20), HEK293T supernatant (starting at 1:4.5), or mAbs (starting at
363 10μg/ml) were mixed with pseudoviruses at 37˚C for 1hr. HEK293T-hACE2 cells
364 (1.5×10^4 per well) were added into the mixture and incubated at 37˚C for 48hrs. Cells
365 were lysed to measure luciferase activity by Bright-Lite Luciferase Assay System
366 (Vazyme Biotech, DD1204-02). The percentages of neutralization were determined by
367 comparing with the virus control. The plasmids encoding spike of WT, Alpha, Beta,
368 Gamma, Delta, BA.1, BA.4/5, XBB, XBB.1.5 and SARS-CoV-1 were kindly provided
369 by Prof. Linqi Zhang at Tsinghua University. The plasmids encoding spike of BA.2.75
370 was kindly provided by Prof. Zezhong Liu at Fudan University. The sequences of EG.5,
371 EG.5.1, FL.1.5, FL.1.5.1, HK.3, BA.2.86 and JN.1 spike were synthesized and cloned
372 into expression vectors.

373 **Competition ELISA**

374 NTD-specific and RBD-specific neutralizing mAbs were labeled with HRP (ProteinTech,
375 PK20001). XBB.1.5 spike was coated onto 96-well ELISA plates (50 ng/well) and
376 incubated at 4˚C overnight. After blocking with PBS containing 10% FBS, blocking
377 mAbs were added to the wells and incubated at 37˚C for 1hr. HRP-labeled detecting
378 mAbs were added to the wells in the presence of competing mAbs. The ratio of
379 blocking antibody and detecting antibody is 100:1. After 1hr incubation at 37˚C, TMB
380 substrate (Sangon Biotech, E661007-0100) was added to the wells and incubated at
381 room temperature for 30 mins. The reaction was stopped by TMB Stop Solution
382 (Sangon Biotech, E661006-0500) and absorbance at 450 nm were measured. The
383 percentages of signal decrease caused by blocking mAbs were calculated.

384 **ACE2 competition FACS**

385 5nM biotinylated XBB.1.5 spike was incubated with 10μg/ml competing mAbs for
386 30min at 4˚C, then the mixtures were added to HEK293T-hACE2 cells. After 30min at
387 4˚C, the cells were washed with FACS buffer. Streptavidin-APC (BioLegend, 405207)
388 and DAPI were added to the wells at 4˚C for 30min. The stained cells were washed
389 with FACS buffer and resuspended in 200μl FACS buffer. Positive cells were gated as
390 $DAPI^{-}$XBB.1.5 $spike^{+}$. The percentages of signal decrease caused by competing mAbs
391 were calculated.

392 **Germline antibodies binding FACS**

393 The plasmids encoding spikes of SARS-CoV-2 WT, Alpha, Beta, Gamma, Delta, BA.1,
394 BA.4/5, BF.7, BA.2.75, BQ.1, XBB.1.5, EG.5.1, BA.2.86 were transfected into
395 HEK293T cells. After 48hr, cells were harvested and incubated with 50μg/ml germline

396 antibodies for 30min at 4˚C. After washed with FACS buffer, cells were stained with
397 goat anti-human IgG FITC (Proteintech, SA00003-12) and DAPI. The stained cells
398 were washed with FACS buffer and resuspended in 200μl FACS buffer. Positive cells
399 were gated as $DAPI^{-}IgG^{+}$.

400 **Acknowledgements**

401 The authors thank all donors for providing peripheral blood. This work was supported
402 by the National Key Plan for Scientific Research and Development of China (Grant No.
403 2022YFC2305800) and the National Natural Science Foundation of China (Grant No.
404 32200765, Grant No. 32370941).

405 **Author contributions**

406 Conceptualization, L.J. and T.Z.; Methodology, L.J. and T.Z.; Validation, Z.W., L.L., R.D.,
407 X.C., Y.S.; Formal Analysis, Z.W.; Investigation, Z.W., L.L., R.D., X.C., Y.S., R.Q., Y.L.,
408 H.F., L.H., X.C., M.L., L.J. and T.Z.; Writing – Original Draft, L.J. and T.Z.; Writing –
409 Review & Editing, L.J., T.Z., Z.W., L.L.; Visualization, T.Z., Z.W.; Supervision, L.J. and
410 T.Z.; Funding Acquisition, L.J. and T.Z.;

411 **Competing interests**

412 L.J., T.Z., L.L. and Z.W. are inventors on a patent application for antibodies including
413 KXD-E1, KXD-F1, KXD-F3, KXD-G5 and KXD-G10. The other authors declare that
414 they have no competing interests.

415 **Supplemental information**

416 Figures S1–S3 and Table S1

417 Data S1. Excel spreadsheet containing numerical data for figures.

418 **Figure legends**

419 **Figure 1. Sequential Omicron infections could not overcome ancestral SARS-**
420 **CoV-2 immune imprinting induced by inactivated or recombinant RBD vaccines.**
421 (A) Vaccination and infection information of 12 donors. (B, C) Summary of plasma
422 neutralizing antibody titers (NT50). For plasma with no neutralizing activity at 20-fold
423 dilution, a number between 10–20 is given as titer to separate the curves. The numbers
424 below the line are geometric mean titers against the pseudoviruses. The titers against
425 WT are compared with other variants and the fold changes are indicated above the
426 line. For panel B, statistical analysis was performed by two-tailed paired T test. For
427 panel C, statistical analysis was performed by two-tailed Wilcoxon matched-pairs
428 signed rank test. *P < 0.05, **P < 0.01, **** P < 0.0001. (D) Comparison of neutralizing
429 antibody titers of G1 (Donor A-D, unimprinted group) and G2 (Donor E-K, imprinted
430 group). The numbers on top are fold changes. Statistical analysis was performed by
431 two-tailed unpaired T test. *P < 0.05, **P < 0.01. The neutralizing titers are calculated
432 with results from two independent experiments, in which duplicates are performed.

433 **Figure 2. Immune imprinting leads to more frequent cross-reactive antibodies to**
434 **RBD but not NTD.** (A) ELISA and neutralization results of 364 mAbs. Supernatant of
435 HEK293T cells was tested against Spike, S1, S2, NTD and RBD of WT and XBB.1.5
436 by ELISA, and tested against WT and XBB.1.5. pseudoviruses by neutralization assay.
437 For ELISA, supernatant was not diluted. For neutralization, supernatant was diluted by
438 4.5-fold. The results are mean values of two independent experiments. For
439 neutralization, duplicates are performed in each experiment. (B) Frequency of binding

440 mAbs and neutralizing mAbs against different domains in each individual. (C)
441 Frequencies of WT-cross-reactive antibodies (XBB.1.5^{+} WT^{+}) and Omicron-specific
442 antibodies (XBB.1.5^{+} WT^{-}) in each individual. (D) Comparison of WT-cross-reactive
443 antibodies between G1 and G2. Data are represented as mean ± SD. Statistical
444 analysis was performed by two-tailed unpaired T test. NS (Not significant) $p > 0.05$, **P
445 < 0.01.

446 **Figure 3. Immune imprinting facilitates the development of broadly neutralizing**
447 **antibodies against RBD.** (A) IC50s of mAbs against WT, Alpha, Beta, Gamma, Delta,
448 BA.1, BA.4/5, BA.2.75, BQ.1, XBB, XBB.1.5, EG.5.1, HK.3, BA.2.86 and JN.1. The
449 highest antibody concentration used to determine IC50 is 10μg/ml. (B) Comparing
450 IC50s of RBD-specific mAbs from three groups. (C) Comparing IC50s of NTD-specific
451 mAbs from two groups. Data are represented as the mean ± SD. Statistical analysis
452 was performed by two-tailed unpaired T test. NS (Not significant) $p > 0.05$, *P < 0.05,
453 **P < 0.01. IC50s are calculated with results from two independent experiments, in
454 which duplicates are performed.

455 **Figure 4. Repeated Omicron infections induce de novo Omicron-specific**
456 **antibody responses in the presence of immune imprinting.** (A) Binding
457 specificities of germline antibodies measured by FACS. HEK293T cells expressing
458 SARS-CoV-2 spikes were incubated with 50μg/ml germline antibodies and analyzed
459 by FACS. The percentages of positive cells are calculated. The results are mean
460 values of two independent experiments. (B) Somatic hypermutations of VH and VL.
461 DNA sequences were analyzed. Data are represented as mean ± SD. Statistical

462 analysis was performed by two-tailed unpaired T test. NS (Not significant) $p > 0.05$, **P
463 < 0.01, ***P < 0.001, ****P < 0.0001. (C) Frequencies of V genes in each group.
464 Frequently used V genes are highlighted by colored background.

465 **Figure 5. Omicron-specific and WT-cross-reactive antibodies recognize similar**
466 **epitopes.** (A) Competition ELISA of RBD-specific mAbs. Competition with ACE2 was
467 performed by FACS. (B) Competition ELISA of NTD-specific mAbs. The results are
468 mean values of two independent experiments.

469 **Figure S1. Plasma neutralizing antibody titers.** (A) Measurement of neutralizing
470 antibody titers against a panel of pseudoviruses. Data are represented as mean ± SD.
471 (B) Neutralizing antibody titers of donor L.

472 **Figure S2. FACS plots representing gating strategies for XBB.1.5 spike-specific**
473 **single B cell sorting.**

474 **Figure S3. Neutralizing potency of mAbs against different variants.** (A) IC50s of
475 RBD-specific mAbs. The numbers below the line are geometric mean IC50 of mAbs
476 against the pseudoviruses. IC50s against BA.4/5 are compared with other variants. (B)
477 IC50s of NTD-specific mAbs. The numbers below the line are geometric mean IC50 of
478 mAbs against the pseudoviruses. IC50s against XBB are compared other variants.
479 Statistical analysis was performed by two-tailed Wilcoxon matched-pairs signed rank
480 test. NS (Not significant) $p > 0.05$, *P < 0.05, **P < 0.01, ***P < 0.001, ****P < 0.0001.
481

482 **References**

483 1. Gray, D. (1993). Immunological memory. Annu Rev Immunol *11*, 49-77.
484 10.1146/annurev.iy.11.040193.000405.
485 2. Victora, G.D., and Nussenzweig, M.C. (2022). Germinal Centers. Annu Rev Immunol *40*,
486 413-442. 10.1146/annurev-immunol-120419-022408.
487 3. Mesin, L., Schiepers, A., Ersching, J., Barbulescu, A., Cavazzoni, C.B., Angelini, A., Okada, T.,
488 Kurosaki, T., and Victora, G.D. (2020). Restricted Clonality and Limited Germinal Center
489 Reentry Characterize Memory B Cell Reactivation by Boosting. Cell *180*, 92-106 e111.
490 10.1016/j.cell.2019.11.032.
491 4. Francis, T. (1960). On the Doctrine of Original Antigenic Sin. Proceedings of the American
492 Philosophical Society *104*, 572-578.
493 5. Viana, R., Moyo, S., Amoako, D.G., Tegally, H., Scheepers, C., Althaus, C.L., Anyaneji, U.J.,
494 Bester, P.A., Boni, M.F., Chand, M., et al. (2022). Rapid epidemic expansion of the SARS-
495 CoV-2 Omicron variant in southern Africa. Nature *603*, 679-686. 10.1038/s41586-022-
496 04411-y.
497 6. He, Q., Wu, L., Xu, Z., Wang, X., Xie, Y., Chai, Y., Zheng, A., Zhou, J., Qiao, S., Huang, M., et
498 al. (2023). An updated atlas of antibody evasion by SARS-CoV-2 Omicron sub-variants
499 including BQ.1.1 and XBB. Cell Rep Med *4*, 100991. 10.1016/j.xcrm.2023.100991.
500 7. Kurhade, C., Zou, J., Xia, H., Liu, M., Chang, H.C., Ren, P., Xie, X., and Shi, P.Y. (2023). Low
501 neutralization of SARS-CoV-2 Omicron BA.2.75.2, BQ.1.1 and XBB.1 by parental mRNA
502 vaccine or a BA.5 bivalent booster. Nat Med *29*, 344-347. 10.1038/s41591-022-02162-x.
503 8. Wang, Q., Iketani, S., Li, Z., Liu, L., Guo, Y., Huang, Y., Bowen, A.D., Liu, M., Wang, M., Yu,
504 J., et al. (2023). Alarming antibody evasion properties of rising SARS-CoV-2 BQ and XBB
505 subvariants. Cell *186*, 279-286 e278. 10.1016/j.cell.2022.12.018.
506 9. Miller, J., Hachmann, N.P., Collier, A.Y., Lasrado, N., Mazurek, C.R., Patio, R.C., Powers, O.,
507 Surve, N., Theiler, J., Korber, B., and Barouch, D.H. (2023). Substantial Neutralization
508 Escape by SARS-CoV-2 Omicron Variants BQ.1.1 and XBB.1. N Engl J Med *388*, 662-664.
509 10.1056/NEJMc2214314.
510 10. Wang, Q., Guo, Y., Zhang, R.M., Ho, J., Mohri, H., Valdez, R., Manthei, D.M., Gordon, A.,
511 Liu, L., and Ho, D.D. (2023). Antibody neutralisation of emerging SARS-CoV-2 subvariants:
512 EG.5.1 and XBC.1.6. Lancet Infect Dis *23*, e397-e398. 10.1016/S1473-3099(23)00555-8.
513 11. Yang, S., Yu, Y., Xu, Y., Jian, F., Song, W., Yisimayi, A., Wang, P., Wang, J., Liu, J., Yu, L., et
514 al. (2024). Fast evolution of SARS-CoV-2 BA.2.86 to JN.1 under heavy immune pressure.
515 Lancet Infect Dis *24*, e70-e72. 10.1016/S1473-3099(23)00744-2.
516 12. Chalkias, S., Eder, F., Essink, B., Khetan, S., Nestorova, B., Feng, J., Chen, X., Chang, Y., Zhou,
517 H., Montefiori, D., et al. (2022). Safety, immunogenicity and antibody persistence of a
518 bivalent Beta-containing booster vaccine against COVID-19: a phase 2/3 trial. Nat Med
519 *28*, 2388-2397. 10.1038/s41591-022-02031-7.
520 13. Chalkias, S., Harper, C., Vrbicky, K., Walsh, S.R., Essink, B., Brosz, A., McGhee, N., Tomassini,
521 J.E., Chen, X., Chang, Y., et al. (2022). A Bivalent Omicron-Containing Booster Vaccine
522 against Covid-19. N Engl J Med *387*, 1279-1291. 10.1056/NEJMoa2208343.
523 14. Collier, A.Y., Miller, J., Hachmann, N.P., McMahan, K., Liu, J., Bondzie, E.A., Gallup, L., Rowe,
524 M., Schonberg, E., Thai, S., et al. (2023). Immunogenicity of BA.5 Bivalent mRNA Vaccine

525 Boosters. N Engl J Med *388*, 565-567. 10.1056/NEJMc2213948.
526 15. Park, Y.J., Pinto, D., Walls, A.C., Liu, Z., De Marco, A., Benigni, F., Zatta, F., Silacci-Fregni, C.,
527 Bassi, J., Sprouse, K.R., et al. (2022). Imprinted antibody responses against SARS-CoV-2
528 Omicron sublineages. Science *378*, 619-627. 10.1126/science.adc9127.
529 16. Wang, Z., Zhou, P., Muecksch, F., Cho, A., Ben Tanfous, T., Canis, M., Witte, L., Johnson, B.,
530 Raspe, R., Schmidt, F., et al. (2022). Memory B cell responses to Omicron subvariants after
531 SARS-CoV-2 mRNA breakthrough infection in humans. J Exp Med *219*.
532 10.1084/jem.20221006.
533 17. Kaku, C.I., Bergeron, A.J., Ahlm, C., Normark, J., Sakharkar, M., Forsell, M.N.E., and Walker,
534 L.M. (2022). Recall of preexisting cross-reactive B cell memory after Omicron BA.1
535 breakthrough infection. Sci Immunol *7*, eabq3511. 10.1126/sciimmunol.abq3511.
536 18. Quandt, J., Muik, A., Salisch, N., Lui, B.G., Lutz, S., Kruger, K., Wallisch, A.K., Adams-Quack,
537 P., Bacher, M., Finlayson, A., et al. (2022). Omicron BA.1 breakthrough infection drives
538 cross-variant neutralization and memory B cell formation against conserved epitopes. Sci
539 Immunol *7*, eabq2427. 10.1126/sciimmunol.abq2427.
540 19. Weber, T., Dahling, S., Rose, S., Affeldt, P., Vanshylla, K., Ullrich, L., Gieselmann, L., Teipel,
541 F., Gruell, H., Di Cristanziano, V., et al. (2023). Enhanced SARS-CoV-2 humoral immunity
542 following breakthrough infection builds upon the preexisting memory B cell pool. Sci
543 Immunol *8*, eadk5845. 10.1126/sciimmunol.adk5845.
544 20. Addetia, A., Piccoli, L., Case, J.B., Park, Y.J., Beltramello, M., Guarino, B., Dang, H., de Melo,
545 G.D., Pinto, D., Sprouse, K., et al. (2023). Neutralization, effector function and immune
546 imprinting of Omicron variants. Nature *621*, 592-601. 10.1038/s41586-023-06487-6.
547 21. Wang, Q., Guo, Y., Tam, A.R., Valdez, R., Gordon, A., Liu, L., and Ho, D.D. (2023). Deep
548 immunological imprinting due to the ancestral spike in the current bivalent COVID-19
549 vaccine. Cell Rep Med *4*, 101258. 10.1016/j.xcrm.2023.101258.
550 22. Yisimayi, A., Song, W., Wang, J., Jian, F., Yu, Y., Chen, X., Xu, Y., Yang, S., Niu, X., Xiao, T.,
551 et al. (2024). Repeated Omicron exposures override ancestral SARS-CoV-2 immune
552 imprinting. Nature *625*, 148-156. 10.1038/s41586-023-06753-7.
553 23. Johnston, T.S., Li, S.H., Painter, M.M., Atkinson, R.K., Douek, N.R., Reeg, D.B., Douek, D.C.,
554 Wherry, E.J., and Hensley, S.E. (2024). Immunological imprinting shapes the specificity of
555 human antibody responses against SARS-CoV-2 variants. Immunity *57*, 912-925 e914.
556 10.1016/j.immuni.2024.02.017.
557 24. Tortorici, M.A., Addetia, A., Seo, A.J., Brown, J., Sprouse, K., Logue, J., Clark, E., Franko, N.,
558 Chu, H., and Veesler, D. (2024). Persistent immune imprinting occurs after vaccination with
559 the COVID-19 XBB.1.5 mRNA booster in humans. Immunity *57*, 904-911 e904.
560 10.1016/j.immuni.2024.02.016.
561 25. Liang, C.Y., Raju, S., Liu, Z., Li, Y., Asthagiri Arunkumar, G., Case, J.B., Scheaffer, S.M., Zost,
562 S.J., Acreman, C.M., Gagne, M., et al. (2024). Imprinting of serum neutralizing antibodies
563 by Wuhan-1 mRNA vaccines. Nature. 10.1038/s41586-024-07539-1.
564 26. Pan, Y., Wang, L., Feng, Z., Xu, H., Li, F., Shen, Y., Zhang, D., Liu, W.J., Gao, G.F., and Wang,
565 Q. (2023). Characterisation of SARS-CoV-2 variants in Beijing during 2022: an
566 epidemiological and phylogenetic analysis. Lancet *401*, 664-672. 10.1016/S0140-
567 6736(23)00129-0.
568 27. Feng, Y., Su, Q., Li, L., He, X., Niu, P., Guo, X., Zhao, X., Tang, J., Jia, Z., and Wang, J. (2024).

569 Genomic Surveillance for SARS-CoV-2 Variants: Dominance of XBB Replacement—China,
570 January–June 2023. China CDC Weekly *6*, 324-331.
571 28. Wang, Y., Yuan, M., Lv, H., Peng, J., Wilson, I.A., and Wu, N.C. (2022). A large-scale
572 systematic survey reveals recurring molecular features of public antibody responses to
573 SARS-CoV-2. Immunity *55*, 1105-1117 e1104. 10.1016/j.immuni.2022.03.019.
574 29. Yan, Q., Hou, R., Huang, X., Zhang, Y., He, P., Zhang, Y., Liu, B., Wang, Q., Rao, H., Chen,
575 X., et al. (2022). Shared IGHV1-69-encoded neutralizing antibodies contribute to the
576 emergence of L452R substitution in SARS-CoV-2 variants. Emerg Microbes Infect *11*,
577 2749-2761. 10.1080/22221751.2022.2140611.
578 30. Cao, Y., Jian, F., Wang, J., Yu, Y., Song, W., Yisimayi, A., Wang, J., An, R., Chen, X., Zhang,
579 N., et al. (2023). Imprinted SARS-CoV-2 humoral immunity induces convergent Omicron
580 RBD evolution. Nature *614*, 521-529. 10.1038/s41586-022-05644-7.
581 31. Koutsakos, M., and Ellebedy, A.H. (2023). Immunological imprinting: Understanding
582 COVID-19. Immunity *56*, 909-913. 10.1016/j.immuni.2023.04.012.
583 32. Walls, A.C., Park, Y.J., Tortorici, M.A., Wall, A., McGuire, A.T., and Veesler, D. (2020).
584 Structure, Function, and Antigenicity of the SARS-CoV-2 Spike Glycoprotein. Cell *181*,
585 281-292 e286. 10.1016/j.cell.2020.02.058.
586 33. Wrapp, D., Wang, N., Corbett, K.S., Goldsmith, J.A., Hsieh, C.L., Abiona, O., Graham, B.S.,
587 and McLellan, J.S. (2020). Cryo-EM structure of the 2019-nCoV spike in the prefusion
588 conformation. Science *367*, 1260-1263. 10.1126/science.abb2507.
589 34. Chi, X., Yan, R., Zhang, J., Zhang, G., Zhang, Y., Hao, M., Zhang, Z., Fan, P., Dong, Y., Yang,
590 Y., et al. (2020). A neutralizing human antibody binds to the N-terminal domain of the
591 Spike protein of SARS-CoV-2. Science *369*, 650-655. 10.1126/science.abc6952.
592 35. Liu, L., Wang, P., Nair, M.S., Yu, J., Rapp, M., Wang, Q., Luo, Y., Chan, J.F., Sahi, V., Figueroa,
593 A., et al. (2020). Potent neutralizing antibodies against multiple epitopes on SARS-CoV-2
594 spike. Nature *584*, 450-456. 10.1038/s41586-020-2571-7.
595 36. McCallum, M., De Marco, A., Lempp, F.A., Tortorici, M.A., Pinto, D., Walls, A.C., Beltramello,
596 M., Chen, A., Liu, Z., Zatta, F., et al. (2021). N-terminal domain antigenic mapping reveals
597 a site of vulnerability for SARS-CoV-2. Cell *184*, 2332-2347 e2316.
598 10.1016/j.cell.2021.03.028.
599 37. Suryadevara, N., Shrihari, S., Gilchuk, P., VanBlargan, L.A., Binshtein, E., Zost, S.J., Nargi,
600 R.S., Sutton, R.E., Winkler, E.S., Chen, E.C., et al. (2021). Neutralizing and protective human
601 monoclonal antibodies recognizing the N-terminal domain of the SARS-CoV-2 spike
602 protein. Cell *184*, 2316-2331 e2315. 10.1016/j.cell.2021.03.029.
603 38. Wang, Z., Muecksch, F., Cho, A., Gaebler, C., Hoffmann, H.H., Ramos, V., Zong, S., Cipolla,
604 M., Johnson, B., Schmidt, F., et al. (2022). Analysis of memory B cells identifies conserved
605 neutralizing epitopes on the N-terminal domain of variant SARS-Cov-2 spike proteins.
606 Immunity *55*, 998-1012 e1018. 10.1016/j.immuni.2022.04.003.
607 39. Cerutti, G., Guo, Y., Wang, P., Nair, M.S., Wang, M., Huang, Y., Yu, J., Liu, L., Katsamba, P.S.,
608 Bahna, F., et al. (2021). Neutralizing antibody 5-7 defines a distinct site of vulnerability in
609 SARS-CoV-2 spike N-terminal domain. Cell Rep *37*, 109928.
610 10.1016/j.celrep.2021.109928.
611 40. Li, L., Chen, X., Wang, Z., Li, Y., Wang, C., Jiang, L., and Zuo, T. (2023). Breakthrough
612 infection elicits hypermutated IGHV3-53/3-66 public antibodies with broad and potent

613 neutralizing activity against SARS-CoV-2 variants including the emerging EG.5 lineages.
614 PLoS Pathog *19*, e1011856. 10.1371/journal.ppat.1011856.
615 41. Ju, B., Zhang, Q., Wang, Z., Aw, Z.Q., Chen, P., Zhou, B., Wang, R., Ge, X., Lv, Q., Cheng, L.,
616 et al. (2023). Infection with wild-type SARS-CoV-2 elicits broadly neutralizing and
617 protective antibodies against omicron subvariants. Nat Immunol *24*, 690-699.
618 10.1038/s41590-023-01449-6.
619 42. Liu, Y., Wang, Z., Zhuang, X., Zhang, S., Chen, Z., Zou, Y., Sheng, J., Li, T., Tai, W., Yu, J., et
620 al. (2023). Inactivated vaccine-elicited potent antibodies can broadly neutralize SARS-
621 CoV-2 circulating variants. Nat Commun *14*, 2179. 10.1038/s41467-023-37926-7.
622 43. Ju, B., Fan, Q., Liu, C., Shen, S., Wang, M., Guo, H., Zhou, B., Ge, X., and Zhang, Z. (2023).
623 Omicron BQ.1.1 and XBB.1 unprecedentedly escape broadly neutralizing antibodies
624 elicited by prototype vaccination. Cell Rep *42*, 112532. 10.1016/j.celrep.2023.112532.

625

Figure 1

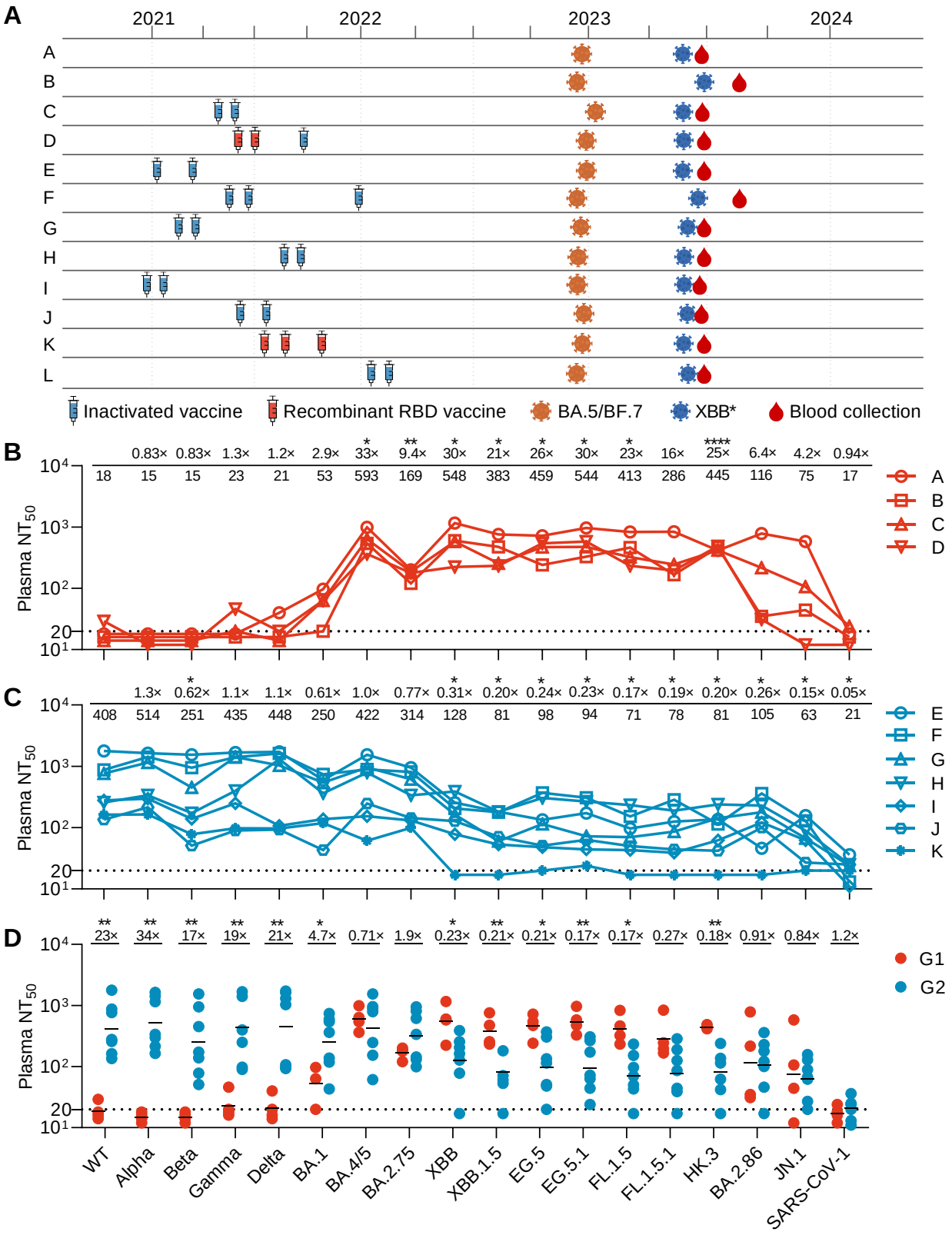
A
2021
2022
2023
2024
A
B
C
D
E
F
G
H
I
J
K
L
Inactivated vaccine
Recombinant RBD vaccine
BA.5/BF.7
XBB*
Blood collection
B
0.83× 0.83× 1.3× 1.2× 2.9× 33× 9.4× 30× 21× 26× 30× 23× 16× 25× 6.4× 4.2× 0.94×
18 15 15 23 21 53 593 169 548 383 459 544 413 286 445 116 75 17
Plasma NT50
A
B
C
D
C
1.3× 0.62× 1.1× 1.1× 0.61× 1.0× 0.77× 0.31× 0.20× 0.24× 0.23× 0.17× 0.19× 0.20× 0.26× 0.15× 0.05×
408 514 251 435 448 250 422 314 128 81 98 94 71 78 81 105 63 21
Plasma NT50
E
F
G
H
I
J
K
D
23× 34× 17× 19× 21× 4.7× 0.71× 1.9× 0.23× 0.21× 0.21× 0.17× 0.17× 0.27× 0.18× 0.91× 0.84× 1.2×
Plasma NT50
G1
G2
WT
Alpha
Beta
Gamma
Delta
BA.1
BA.4/5
BA.2.75
XBB
XBB.1.5
EG.5
EG.5.1
FL.1.5
FL.1.5.1
HK.3
BA.2.86
JN.1
SARS-CoV-1

Figure 2

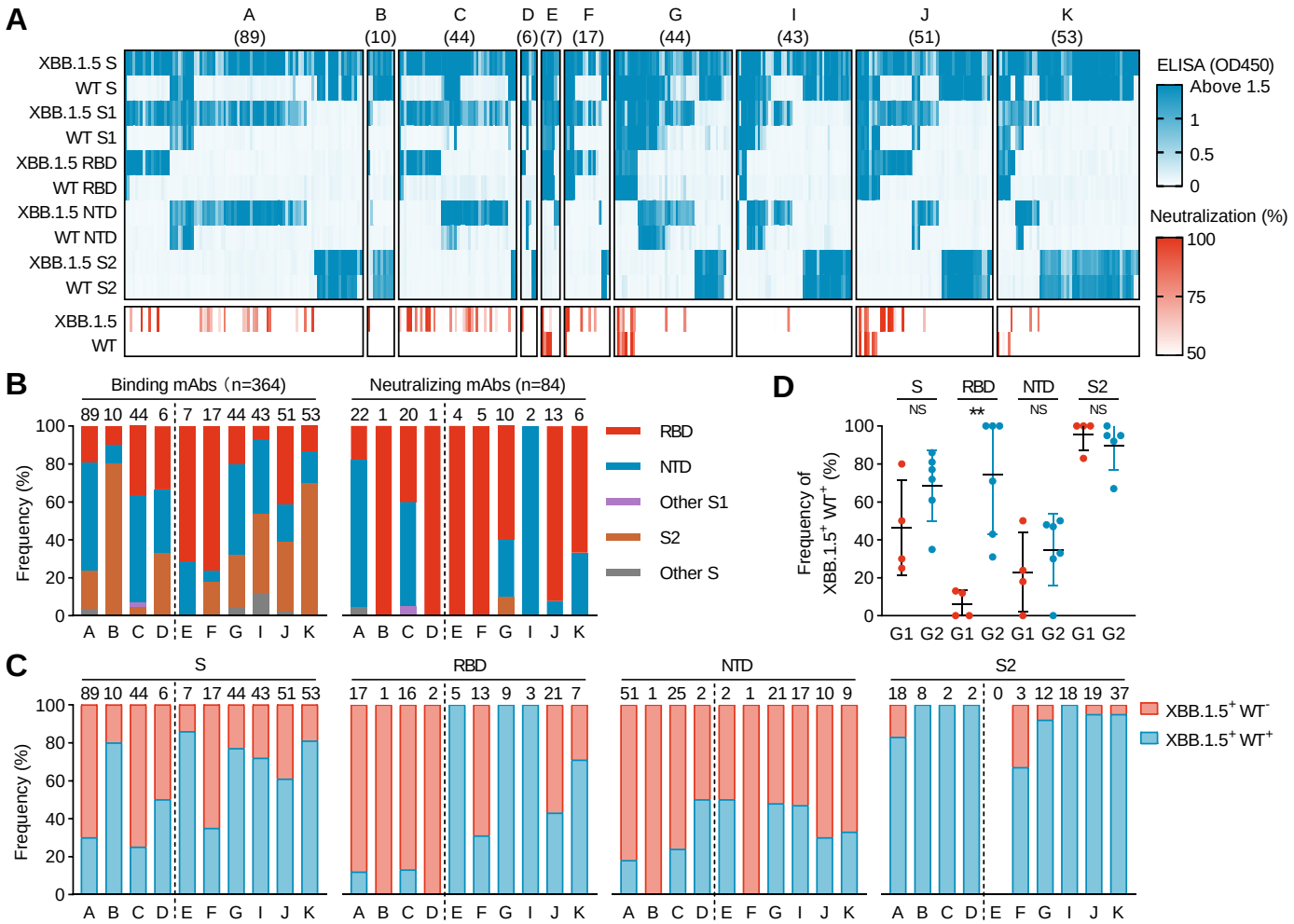
A
A (89)
B (10)
C (44)
D (6)
E (7)
F (17)
G (44)
I (43)
J (51)
K (53)
XBB.1.5 S
WT S
XBB.1.5 S1
WT S1
XBB.1.5 RBD
WT RBD
XBB.1.5 NTD
WT NTD
XBB.1.5 S2
WT S2
XBB.1.5
WT
ELISA (OD450)
Above 1.5
1
0.5
0
Neutralization (%)
100
75
50
B
Binding mAbs（n=364）
Neutralizing mAbs (n=84)
89 10 44 6 7 17 44 43 51 53
22 1 20 1 4 5 10 2 13 6
Frequency (%)
A B C D E F G I J K
RBD
NTD
Other S1
S2
Other S
D
S
RBD
NTD
S2
NS
**
NS
NS
Frequency of XBB.1.5+ WT+ (%)
G1 G2 G1 G2 G1 G2 G1 G2
C
S
RBD
NTD
S2
89 10 44 6 7 17 44 43 51 53
17 1 16 2 5 13 9 3 21 7
51 1 25 2 2 1 21 17 10 9
18 8 2 2 0 3 12 18 19 37
Frequency (%)
A B C D E F G I J K
XBB.1.5+ WT-
XBB.1.5+ WT+

Figure 3

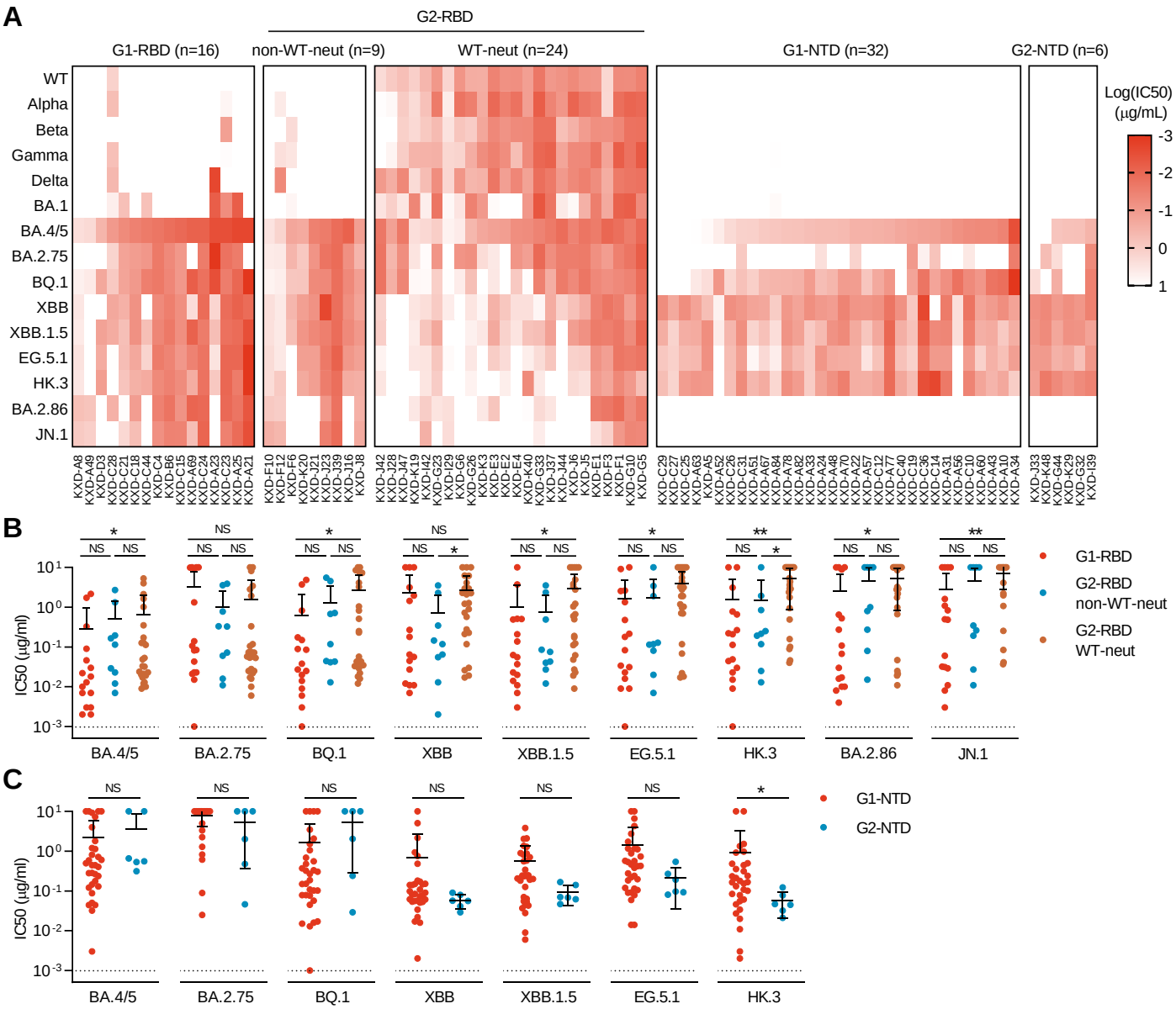
A
G2-RBD
G1-RBD (n=16)
non-WT-neut (n=9)
WT-neut (n=24)
G1-NTD (n=32)
G2-NTD (n=6)
WT
Alpha
Beta
Gamma
Delta
BA.1
BA.4/5
BA.2.75
BQ.1
XBB
XBB.1.5
EG.5.1
HK.3
BA.2.86
JN.1
Log(IC50) (μg/mL)
-3
-2
-1
0
1
B
IC50 (μg/ml)
G1-RBD
G2-RBD non-WT-neut
G2-RBD WT-neut
C
G1-NTD
G2-NTD

Figure 4

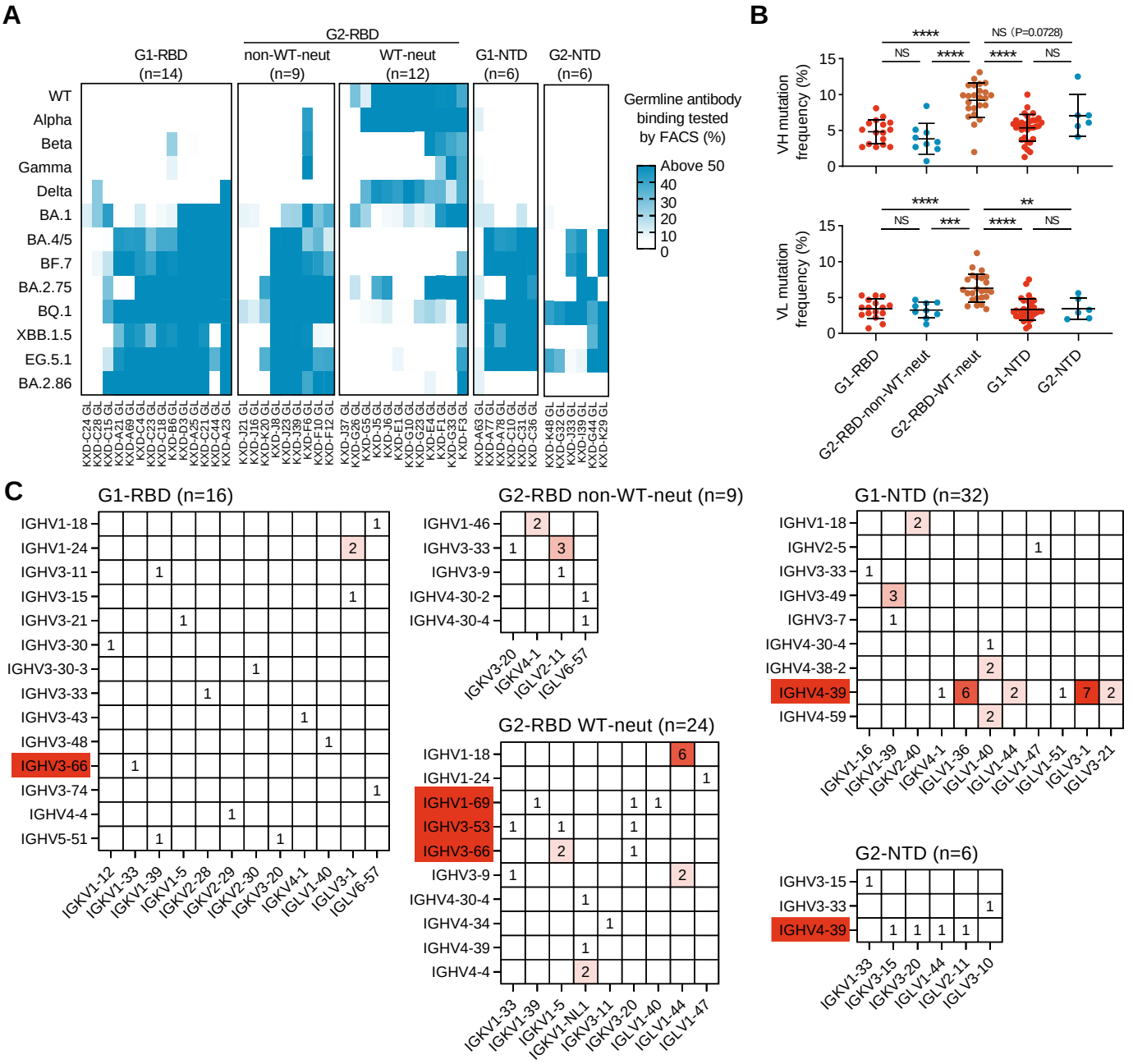
A
G2-RBD
G1-RBD (n=14)
non-WT-neut (n=9)
WT-neut (n=12)
G1-NTD (n=6)
G2-NTD (n=6)
WT
Alpha
Beta
Gamma
Delta
BA.1
BA.4/5
BF.7
BA.2.75
BQ.1
XBB.1.5
EG.5.1
BA.2.86
Germline antibody binding tested by FACS (%)
Above 50
40
30
20
10
0
B
VH mutation frequency (%)
VL mutation frequency (%)
NS (P=0.0728)
NS
****
***
**
G1-RBD
G2-RBD-non-WT-neut
G2-RBD-WT-neut
G1-NTD
G2-NTD
C
G1-RBD (n=16)
G2-RBD non-WT-neut (n=9)
G2-RBD WT-neut (n=24)
G1-NTD (n=32)
G2-NTD (n=6)
IGHV3-66
IGHV1-69
IGHV3-53
IGHV4-39

Figure 5

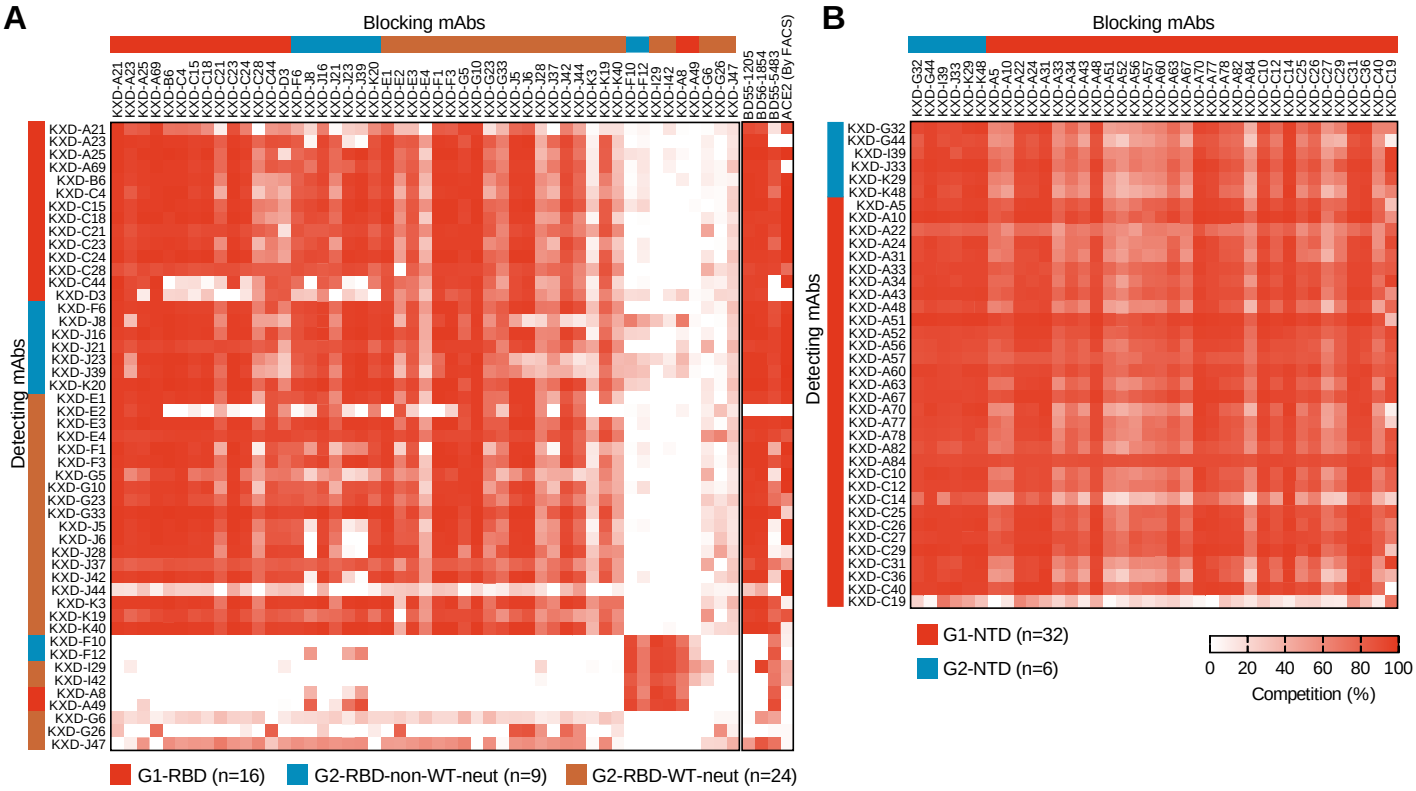
A
Blocking mAbs
Detecting mAbs
BD55-1205
BD56-1854
BD55-5483
ACE2 (by FACS)
G1-RBD (n=16)
G2-RBD-non-WT-neut (n=9)
G2-RBD-WT-neut (n=24)
B
Blocking mAbs
Detecting mAbs
G1-NTD (n=32)
G2-NTD (n=6)
0
20
40
60
80
100
Competition (%)

Figure S1

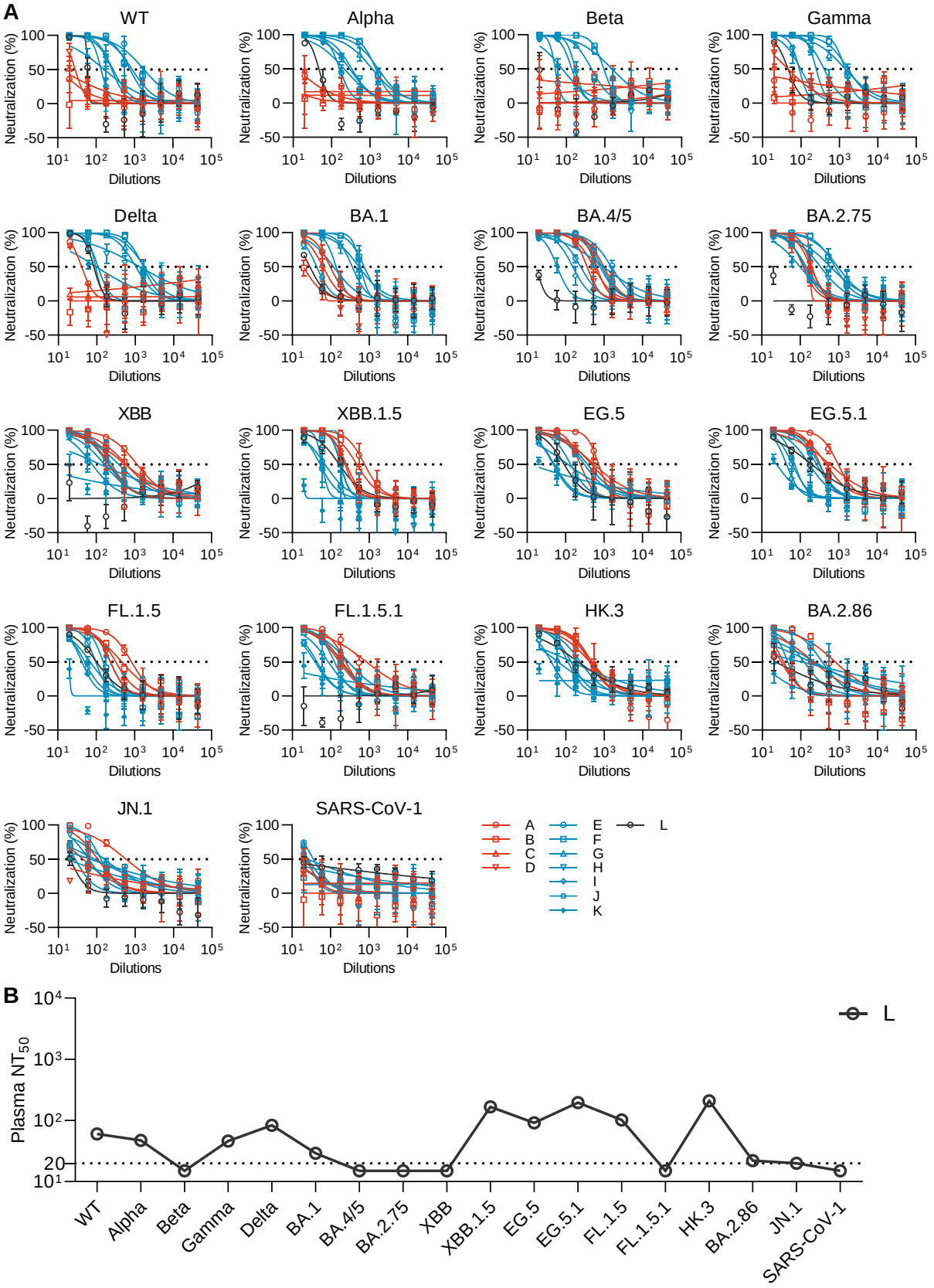
A
WT
Alpha
Beta
Gamma
Delta
BA.1
BA.4/5
BA.2.75
XBB
XBB.1.5
EG.5
EG.5.1
FL.1.5
FL.1.5.1
HK.3
BA.2.86
JN.1
SARS-CoV-1
Neutralization (%)
Dilutions
A
B
C
D
E
F
G
H
I
J
K
L
B
Plasma NT50
WT
Alpha
Beta
Gamma
Delta
BA.1
BA.4/5
BA.2.75
XBB
XBB.1.5
EG.5
EG.5.1
FL.1.5
FL.1.5.1
HK.3
BA.2.86
JN.1
SARS-CoV-1

Figure S2

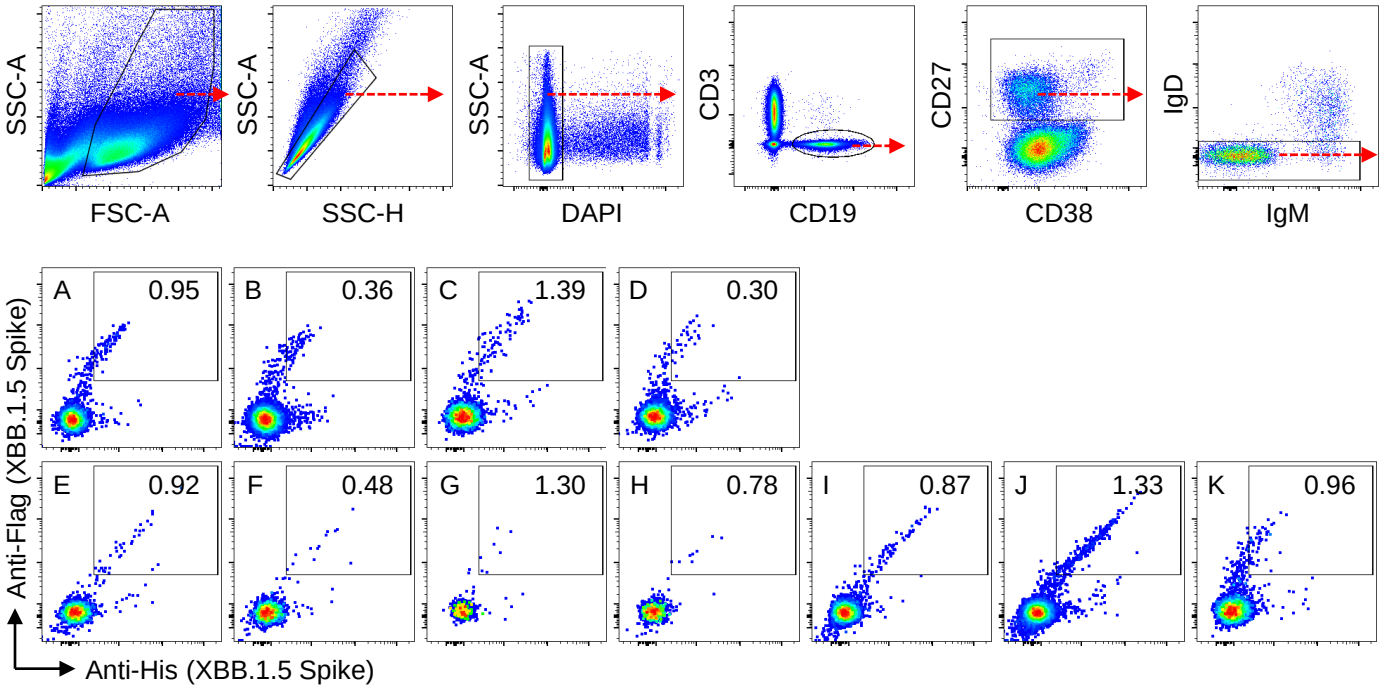
SSC-A
FSC-A
SSC-A
SSC-H
SSC-A
DAPI
CD3
CD19
CD27
CD38
IgD
IgM
A 0.95
B 0.36
C 1.39
D 0.30
E 0.92
F 0.48
G 1.30
H 0.78
I 0.87
J 1.33
K 0.96
Anti-Flag (XBB.1.5 Spike)
Anti-His (XBB.1.5 Spike)

Figure S3

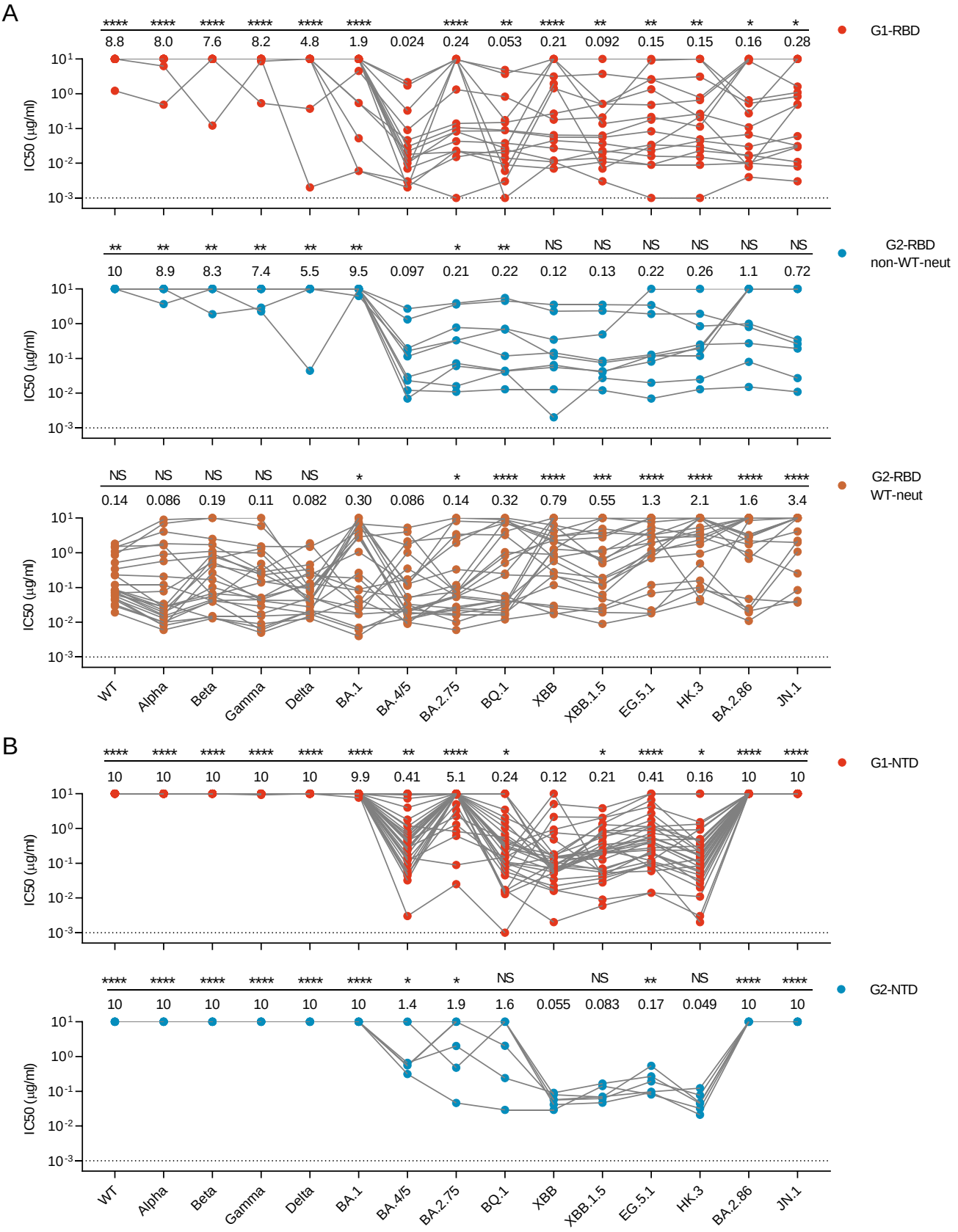
A
G1-RBD
**** **** **** **** **** **** **** ** **** ** ** ** * *
8.8 8.0 7.6 8.2 4.8 1.9 0.024 0.24 0.053 0.21 0.092 0.15 0.15 0.16 0.28
G2-RBD non-WT-neut
** ** ** ** ** ** * ** NS NS NS NS NS NS
10 8.9 8.3 7.4 5.5 9.5 0.097 0.21 0.22 0.12 0.13 0.22 0.26 1.1 0.72
G2-RBD WT-neut
NS NS NS NS NS * * **** **** *** **** **** **** ****
0.14 0.086 0.19 0.11 0.082 0.30 0.086 0.14 0.32 0.79 0.55 1.3 2.1 1.6 3.4
IC50 (µg/ml)
WT Alpha Beta Gamma Delta BA.1 BA.4/5 BA.2.75 BQ.1 XBB XBB.1.5 EG.5.1 HK.3 BA.2.86 JN.1
B
G1-NTD
**** **** **** **** **** **** ** **** * * **** * **** ****
10 10 10 10 10 9.9 0.41 5.1 0.24 0.12 0.21 0.41 0.16 10 10
G2-NTD
**** **** **** **** **** **** * * NS NS ** NS **** ****
10 10 10 10 10 10 1.4 1.9 1.6 0.055 0.083 0.17 0.049 10 10
IC50 (µg/ml)
WT Alpha Beta Gamma Delta BA.1 BA.4/5 BA.2.75 BQ.1 XBB XBB.1.5 EG.5.1 HK.3 BA.2.86 JN.1